Available online at www.sciencedirect.com

ScienceDirect

Procedia Earth and Planetary Science 15 (2015) 125 – 132

Procedia
Earth and Planetary Science

World Multidisciplinary Earth Sciences Symposium, WMESS 2015

Computer Evaluation of Asperity Topology of Rock Joints

Tomáš Ficker[a]*, Dalibor Martišek[b]

[a] *Brno University of Technology, Faculty of Civil Engineering, Department of Physics, Veveří 95, 602 00 Brno, Czech Republic,*
[b] *Brno University of Technology, Faculty of Mechanical Engineering, Department of Mathematics, Technická 2, 616 62 Brno, Czech Republic.*

Abstract

Grounds beneath large civil engineering structures (bridges, dams, tunnels) that are established in the terrain of rock discontinuities represent a risk of mechanical failure. The surface topology of joint surfaces strongly influences shear strength of these discontinuities. It is the asperities that mainly determine the surface topologies and the asperities are characterized by the so-called joint roughness coefficients. In geotechnical practice the joint roughness coefficients are often evaluated visually using ten standard two-dimensional profiles. The visual assessment is rather a subjective procedure but it may be replaced by a computer. The present paper deals with a computerized assessment of joint roughness coefficients. For this purpose the Fourier formalism is employed and works as an expert system recognizing surface topologies.

Peer-review under responsibilty of the Organizing Commitee of WMESS 2015.

Keywords: Rock joints; joint roughness coefficients; Fourier's formalism; indicators of surface topology.

1. Introduction

Terrain instabilities caused by rock joints are serious obstacles for constructions of large civil engineering structures such as bridges, dams or tunnels. The rock joints represent discontinuities in massifs and usually create a three-dimensional network (see Fig. 1). The shear strength of rock discontinuities depends strongly, among others, on surface irregularities of rock joints. The irregularities are formed especially by asperities whose topologies can be characterized by roughness coefficients of various kinds (Ficker et al. 2010), (Ficker, 2011, 2012).

Among various methods assessing asperity topology of rock joints it is the method of Barton and Choubey (1977) that is often used in geotechnical practice. After extensive experimental work these authors presented a model

* Corresponding author. Tel +420 54114 7661.
E-mail address: ficker.t@fce.vutbr.cz

Peer-review under responsibilty of the Organizing Commitee of WMESS 2015.
doi:10.1016/j.proeps.2015.08.031

focused on natural rock joints with irregular asperities. Their model enables to calculate shear strength τ of rock joints as follows

$$\tau = \sigma_n \left[\phi_r + JRC \log\left(\frac{JCS}{\sigma_n} \right) \right] \tag{1}$$

where JRC and JCS are *joint roughness coefficient* and joint compressive strength, respectively. The residual friction angle ϕ_r is equal to the basic friction angle ϕ_b for unweathered rock joints and σ_n is normal stress. The most problematic term in equation (1) is the joint roughness coefficient JRC originally proposed by Barton (1973). To specify values of these coefficients with different rock joints, Barton and Choubey (1977) published 10 standard joint roughness profiles in graphical forms. These two-dimensional profiles correspond to JRC values ranging from zero to twenty with an increment of two, i.e. 0 – 2, 2 – 4, 4 – 6, …. 18 – 20. The authors suggested two possible ways for determining actual JRC values of investigated samples. First, a visual comparison of actual profiles with the ten standards was recommended and, as a second alternative, they suggested a back calculation from tilt and pull tests.

$$JRC = \frac{\arctan(\tau / \sigma_n) - \phi_b}{\log(JCS / \sigma_n)} \tag{2}$$

Fig. 1. The network of rock joints that was uncovered during excavation work at lime quarry Hády near to the city of Brno Czech Republic.

However, the visual comparison is a preferred way for determining JRC-values in geotechnical practice. A quick and easy estimate is probably one of the main reasons for this preference.

The two-dimensional (2D) profiles used for visual assessment are directionally dependent and for this reason, it would be more convenient to use three-dimensional (3D) profiles. In addition, the ten database profiles could be augmented by other standard profiles and this would result in a more detailed database of the standard profiles. Visual assessment of a larger number of 3D profiles may be more difficult and more subjective as compared with the visual assessment of the 2D standard profiles. Thus a computer procedure would be desirable.

The goal of the present paper is to describe a computer procedure that is capable to find two most similar surfaces within a set of numerous 3D surfaces (3D profiles). The computer procedure will be aimed at finding one database surface, which is the most similar to the investigated surface. The database surfaces will be associated with corresponding JRC values and these values will be ascribed to the investigated surfaces on the basis of similarity comparison. To accomplish such a procedure, it is necessary to digitize surfaces and define some numerical indicators of surface similarity. The next section brings possible solutions.

2. Three-dimesnional surface reliefs and indicators of similarity

In order to digitize surfaces whose sizes (5 cm x 3.33 cm) are close to Barton's samples (Barton (1973)), special hardware has been designed and assembled. Its arrangement is shown in Fig. 2. The hardware consists of photographic camera Canon EOS 600D augmented by the objective EF 100mm f/2.8 Macro USM. This objective possesses a sufficiently small depth of optical field when it is set to f/2.8. The photographic camera is mounted on a motorized tough stand, which enables movement in the vertical direction. The vertical stepping movement is governed by the software implemented on the PC. Vertical steps can be set within a wide interval ranging from micrometres up to decimetres, which is far enough to detect height differences of rock asperities. At each vertical position, the camera takes snaps (optical sections) of the surface. The distance between two positions has to be set so that it may not exceed the depth of the optical field of the objective. The depth of optical field should be at least several times smaller than the average height of surface irregularities (asperities). The resulting optical sections serve as input data for software reconstructions of 3D surface reliefs. The main features of the reconstructing software can be found elsewhere (Martišek, 2002). One of the 3D reconstructed reliefs can be seen in Fig. 3.

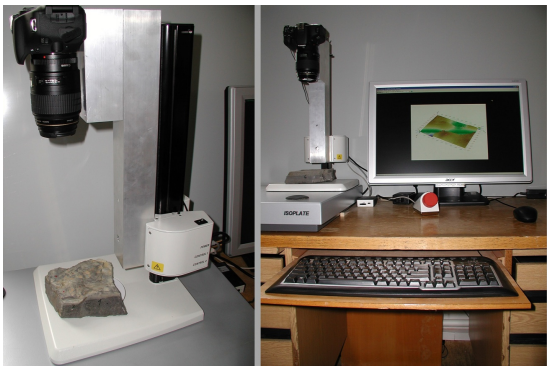

Fig. 2 The hardware for creating optical sections with macroscopic 3D surfaces. The photographic camera Canon EOS 600D is mounted on a vertically movable stand, which is motorized, and controlled by the software implemented on the PC.

The created 3D digital reliefs are further processed using the Fourier expansion to classify numerically wavy shapes of surface profiles. The surface profile can be expressed as a function of two variables $f(x_i, y_j)$ by using the corresponding Fourier series

$$f(x_i,y_j) \approx F_N(x_i,y_j) = \sum_{k,n=0}^{N-1} \lambda_{kn}\left(a_{kn}\cos\frac{k\pi x_i}{p}\cos\frac{n\pi y_j}{q} + b_{kn}\sin\frac{k\pi x_i}{p}\cos\frac{n\pi y_j}{q} + \right.$$
$$\left. + c_{kn}\cos\frac{k\pi x_i}{p}\sin\frac{n\pi y_j}{q} + d_{kn}\sin\frac{k\pi x_i}{p}\sin\frac{n\pi y_j}{q}\right) \tag{3}$$

where

$$\Omega = \{x \in (-p,+p)\,,\, y \in (-q,+q)\} \tag{4}$$

$$a_{kn} = \frac{1}{pq}\iint_\Omega f(x,y)\cos\frac{k\,\pi\,x}{p}\cos\frac{n\,\pi\,y}{q}\,dx\,dy \tag{5}$$

$$b_{kn} = \frac{1}{pq}\iint_\Omega f(x,y)\sin\frac{k\,\pi\,x}{p}\cos\frac{n\,\pi\,y}{q}\,dx\,dy \tag{6}$$

$$c_{kn} = \frac{1}{pq}\iint_{\Omega} f(x,y)\cos\frac{k\pi x}{p}\sin\frac{n\pi y}{q}\,dx\,dy \tag{7}$$

$$d_{kn} = \frac{1}{pq}\iint_{\Omega} f(x,y)\sin\frac{k\pi x}{p}\sin\frac{n\pi y}{q}\,dx\,dy \tag{8}$$

$$\lambda_{kn} = \begin{cases} 1 & (k>0,\, n>0) \\ 1/2 & k=0,\, n>0 \quad or \quad k>0,\, n=0 \\ 1/4 & k=n=0 \end{cases} \tag{9}$$

The symbol *N* defines the upper bound $(N-1)$ for the subscripts n , k and restricts the number of terms in the Fourier sum (3).

We have introduced a matrix $M_N(k,n)$ associated with the Fourier expansion coefficients

$$M_N(k,n) = \sqrt{(\lambda_{k,n}\cdot a_{k,n})^2 + (\lambda_{kn}\cdot b_{k,n})^2 + (\lambda_{k,n}\cdot c_{k,n})^2 + (\lambda_{k,n}\cdot d_{k,n})^2} \tag{10}$$

and a corresponding indicator of shape similarity $S(N)$ as follows

$$S(N) = \sum_{i=0}^{N-1}\sum_{j=0}^{N-1}\frac{|\,M_N^{(o)}(i,j) - M_N(i,j)\,|}{M_N^{(o)}(i,j)} \geq 0 \tag{11}$$

The smaller the value of *S*, the better conformity between compared surfaces can be observed. To enable comparison and quantification of height irregularities of investigated surfaces, a global height parameter is computed, namely the root-mean-square parameter $R_q(N)$ (Ficker et al. 2010), (Ficker, 2011, 2012).

$$R_q(N) = \sqrt{\frac{1}{K\cdot L}\sum_{i=1}^{K}\sum_{j=1}^{L}[f(x_i,y_j) - F_N(x_i,y_j)]^2} \tag{12}$$

where the product $K\cdot L$ is a pixel resolution of the used digital images. In our case $K\cdot L = 720\ pixels \times 480\,\text{pixels}$. The second introduced indicator of similarly is closely related to $R_q(N)$ and quantifies height similarity of surfaces

$$H(N) = \frac{|\,R_q^{(o)}(N) - R_q(N)\,|}{R_q^{(o)}(N)} \geq 0 \tag{13}$$

The smaller the value of *H*, the better agreement between compared surfaces is established. The third introduced indicator of similarity is the correlation coefficient R which evaluates both the height and shape similarities of two surfaces. The surfaces are represented by their discrete 3D reliefs, i.e. discrete matrices C_{ij} , N_{ij} and their mean values $<C_{ij}>, <N_{ij}>$. The graphical form of one of the discrete 3D reliefs is shown in Fig. 3

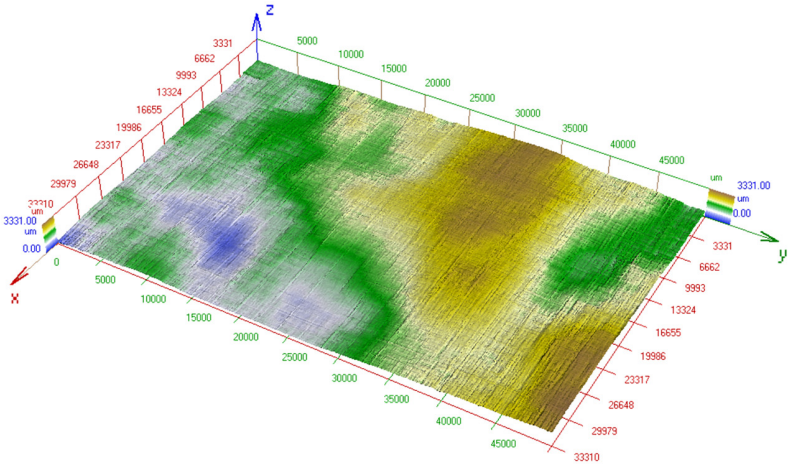

Fig. 3. One of the 3D digital profiles built up from optical sections.

$$R = \frac{\sum_{(i,j)} (C_{ij} - < C_{ij} >)(N_{ij} - < N_{ij} >)}{\sqrt{\left[\sum_{(ij)} (C_{ij} - < C_{ij} >)^2\right]\left[(\sum_{(i,j)} (N_{ij} - < N_{ij} >)^2\right]}} \tag{14}$$

The correlation coefficient R can only assume values from a restricted interval <-1,+1>. The higher the absolute value of R, the better agreement between the surfaces. Two surfaces that have the correlation coefficient equal to +1 or -1 are identical. Although the correlation coefficient R maps height and shape differences of two surfaces, its functioning does not follow that of the former two and as such it is a good complement to the collection of indicators.

In the next section, we will use the three indicators S, H and R to perform comparison between the investigated surface and database surfaces. The couple of the most similar surfaces will contain the database surface whose JRC value will be the best approximation for the JRC value of the investigated surface.

3. Results and discussions

To test the computer method based on the three similarity indicators S, H and R, we have chosen five samples of limestone. Their surfaces showed different stages of irregularities. Three of the samples served as database surfaces and the remaining two were under investigation, i.e. they were compared with the database surfaces. The database surfaces were numbered as 1, 2 and 3 (Fig. 4) whereas the investigated surfaces as A and B (Fig. 5). Both the database and investigated samples were ordered according to their surface irregularities from the rougher to the smoother surfaces. The JRC values of the database surfaces were determined visually according to the Barton standard profiles. To assure a necessary portion of objectivity, we asked 10 persons to determine the database JRC values and then average JRC values and their statistical errors were calculated for all database surfaces:

$$JRC_1 = 18.1 \pm 0.4\,, \quad JRC_2 = 14.9 \pm 0.3\,, \quad JRC_3 = 4.5 \pm 0.3 \tag{15}$$

Similar statistical evaluation was carried out for the investigated surfaces A and B

$$JRC_A = 12 \pm 1\,, \qquad JRC_B = 6.1 \pm 0.7 \tag{16}$$

The closed JRC values between investigated surfaces and those included in the database determine the most similar surfaces. As can be seen from Eqs. (15) and (16), the visual statistical evaluation has suggested two couples of the

most similar surfaces, namely the couples:

A-2 and **B-3**. (17)

Fig. 4 Database surfaces of limestone samples 1, 2 and 3 that serve for similarity comparisons with investigated surfaces. The database JRC values are assigned to the investigated surfaces on the similarity basis.

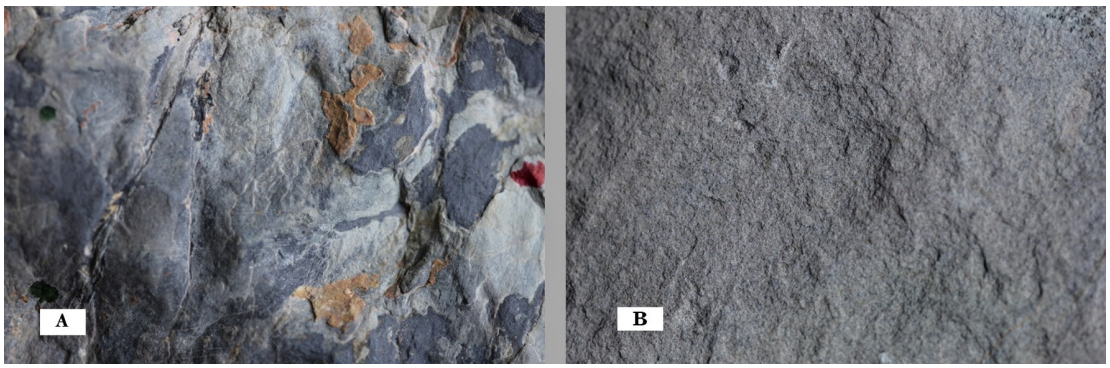

Fig. 5 Investigated surfaces of limestone samples termed as A and B. They serve for similarity tests.

The same comparative test has been performed using the three indicators of similarity *S, H,* and *R*. The results of the comparison between the surface A and the database surfaces 1, 2 and 3 have been graphically plotted and are shown in Fig. 6. The total *minima* of the *S*-indices and *H*-indices unmistakably point toward the database surface no. 2. The total *maximum* of the correlation indices R also points toward the database surface no. 2. In this way the computer procedure has determined the couple **A-2** as a pair of the most similar surfaces and this is in full agreement with the visual evaluation (17).

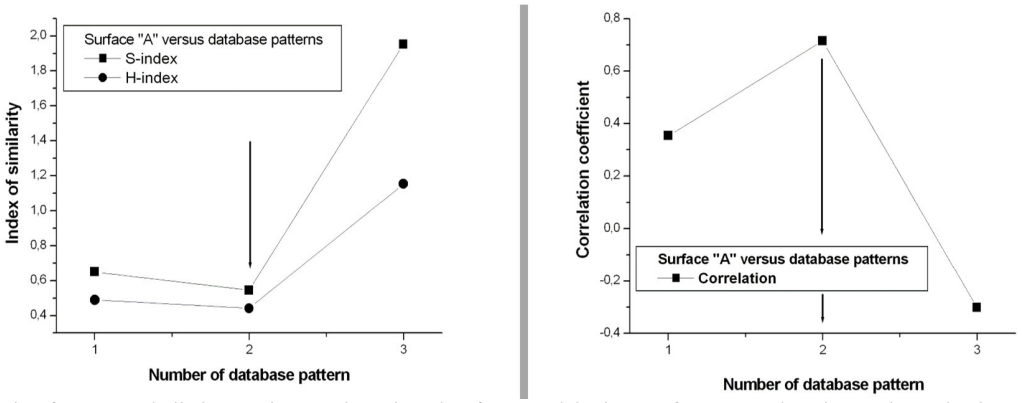

Fig. 6. Results of computer similarity tests between investigated surface A and database surfaces 1, 2 and 3. The couple A-2 has been evaluated as a pair of the most similar surfaces.

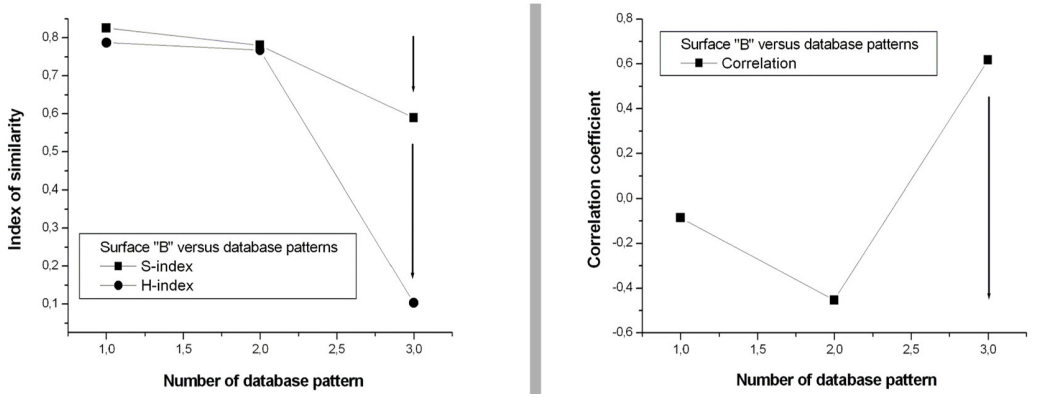

Fig. 7. Results of computer similarity tests between investigated surface B and database surfaces 1, 2 and 3. The couple B-3 has been evaluated as a pair of the most similar surfaces.

The computer comparison of the surface B with the database surfaces 1, 2 and 3 is presented graphically in Fig. 7. The total minima of the S -indices and the H -indices point toward the database surface no. 3. The same result can be observed with the graph of the correlation indices R . The computer procedure is determining the couple **B-3** as the most similar surfaces and this is again in full agreement with the visual evaluation (17).

These tests have indicated that the introduced computer method for recognition of surface similarity possesses a sufficient potential for finding similar surfaces. Because of this similarity comparison, the investigated surfaces A and B may then adopt the database values JRC_1 and JRC_2, respectively. These values are not exactly the same as JRC_A and JRC_B values estimated visually. This is because the software does not determine JRC values directly but only on the similarity basis. If our database contained more standard surfaces, two of which would better coincide with the investigated two surfaces A and B, then the software would point towards the two database surfaces whose JRC values would better coincide with visual estimation. It is seen that it is the quality of the database that is decisive for right determination of JRC values. Anyway, in our case the software has correctly indicated two database surfaces 2 and 3 that are the most similar to the investigated surfaces A and B.

In the case studied the agreement between all the indicators S, H and R has been surprisingly good. However, when the database of standard surfaces is highly populated, slight differences between indicators may appear likewise the differences in visual statistical evaluations (see the statistical uncertainties in Eqs. (15) and (16)). In such cases, average values of JRC might be a solution analogously as the average values with visual assessments (15) and (16). Even weighted averages could be used instead of simple arithmetic averages provided some statistical weights were attributed to the indicators S, H and R . Such possibilities will be studied in due course.

4. Conclusions

In geotechnical practice, the developed computer procedure may be employed as follows. At first, a sufficient number of convenient joint *surfaces* will be collected to form a basis for the database. Then the surfaces will be digitised to create 3D replicas and the corresponding Fourier matrices $M_N(k,n)$ will be computed. The matrices will form a *digital database* that will be incorporated into the software. A next step consists in experimentally determining JRC values of the database surfaces. These values will be calculated according to formula (2). Shear strength τ and basic friction angle ϕ_b (residual angle), which are used in formula (2), will be measured by the shear box apparatus. JCS (joint compressive strength) may be measured by a mechanical press or by the Schmidt hammer. As soon as a permanent database is formed and incorporated into the software together with the corresponding JRC values, the comparison procedure will be ready to use. The optical sections made on the *investigated joint surfaces* will be used as input data for the software. The software will then find one database surface, which is the most similar to the investigated joint surface. The JRC value of the found database surface will

be assigned to the instigated joint surface. This scenario has been illustrated with the present database surfaces 1, 2, and 3 (Fig.4) and the two investigated surfaces A and B (Fig. 5).

Finally, it is possible to summarize as follows. In the present paper, new computer method for recognition of surface similarity has been tested and shown that it has a sufficient potential to determine couples of the most similar surfaces within a set of different surfaces. The computer procedure uses three similarity indicators evaluating shapes, heights and correlation of 3D profiles. The tests carried out with five limestone samples have confirmed consistency between the visual and the computer recognitions. The visual recognition was based on the values averaged over multiple assessments accomplished by 10 independent persons and this supports statistical relevancy of the visual recognition. The computer procedure has provided analogous results with all the similarity indicators. The mutual consistency of both the methods leads us to the conclusion that the computer procedure might become a prospective tool for recognition of surface similarities between rock joints, especially when digital databases of 3D profiles are highly populated.

Acknowledgement

This work was supported by the Grant Agency of the Czech Republic under contract no. 13-03403S. One of us (T.F.) was partly supported on the basis of the grant no. LO 1408 within the program I-LO (NPU I) administered by the Ministry of Education, Youth and Sports of the Czech Republic

References

1. Barton, N., Choubey, V., 1977. The shear strength of rock joints in theory and practice. Rock Mechanics, 10: 1-
2. 65.
3. Barton, N., 1973. Review of a new shear strength criterion for rock joints. Engineering Geology, 7: 87–332.
4. Ficker, T., Martišek, D., Jennings, H. M., 2010. Roughness of fracture surfaces and compressive strength of
5. hydrated cement pastes. Cement and Concrete Research, 40: 947-955.
6. Ficker, T., Martišek, D, 2011. Roughness and fractality of fracture surfaces as indicators of mechanical quantities of porous solids. Central European Journal of Physics, 9: 1440-1445.
7. Ficker, T (2012). Fracture surfaces and compressive strength of hydrated cement pastes. Constructions and Building Materials, **27**, 197-205.
8. Martišek, D., 2002. The two-dimensional and three-dimensional processing of images provided by conventional
9. microscopes. Scanning, 24: 284 – 295.